Charcoal reflectance measurements: Implications for structural characterization and assessment of diagenetic alteration

Philippa L. Ascough*,
SUERC
Scottish Enterprise Technology Park,
Rankine Avenue, East Kilbride G75 0QF, UK

Michael I. Bird
School of Earth and Environmental Sciences
James Cook University PO Box 6811,
Cairns, Queensland, 4870, Australia

Andrew C. Scott, Margaret E. Collinson
Department of Earth Sciences,
Royal Holloway University of London,
Egham, Surrey TW20 OEX, UK

Illit Cohen-Ofri
Weizmann Institute of Science
Rehovot, Israel

Colin E. Snape, Katherine Le Manquais
Fuels and Power Technology Research Division,
University of Nottingham

*corresponding author email: p.ascough@suerc.gla.ac.uk
Present address: SUERC, Scottish Enterprise Technology Park, Rankine Avenue, East Kilbride G75 0QF, UK

Abstract

Charcoal is a valuable source of archaeological and palaeoenvironmental proxy data. However growing evidence suggests that production conditions can strongly influence post-depositional alteration of charcoal. Consequently, both reconstruction of production temperature and understanding of the potential for diagenetic alteration are of great interest. Here, we use mean random reflectance (Ro_{mean}) in conjunction with other chemical characterization methods to address these questions. Ro_{mean} was obtained for a suite of modern analogue charcoal, produced under controlled conditions, and for a series of natural charcoal samples, obtained from archaeological and palaeoenvironmental deposits. Ro_{mean} proves to be a robust measure to assess formation temperature for samples produced at 400°C and above, even after exposure to highly oxidizing conditions. Ro_{mean} is also useful for samples formed between 300°C and 400°C. However, if an assemblage of charcoals has been exposed to oxidizing conditions, lower temperature charcoals may be preferentially lost. It is apparent that charcoal produced at lower temperatures is more highly susceptible to chemical oxidation, and that there is a continuum in charcoal degradation potential, dependant upon fuel material and production conditions.

Keywords

Charcoal, Reflectance, Oxidative degradation, Black Carbon, Diagenesis

Introduction

Charcoal production involves exposure of biomass to elevated temperatures under conditions of restricted oxygen, and is among the oldest forms of human chemical technology (e.g. Moore, 2000). During production, the most prominent chemical change is reorganization of lignocellulosic structures into highly stable condensed polyaromatic configurations (Darmstadt et al., 2000; Eckmeier et al., 2007). Charcoal is consequently among the forms of environmental carbon most resistant to alteration and degradation (Levine, 1991; Preston and Schmidt, 2006), displaying remarkable persistence within the geological record (Pessenda et al., 1996; Collinson et al., 2000; Gouveia et al., 2002; Scott 1989, 2000, 2009; Scott and Glasspool, 2007). Charcoal therefore forms a valuable source of geological, archaeological and palaeoenvironmental proxy data (Scott, 2010), not least as one of the most common materials submitted for radiocarbon (^{14}C) age measurement (Bird, 2006).

Long-term preservation makes it tempting to consider charcoal as chemically homogeneous, and uniformly recalcitrant. However, charcoal is neither a pure form of carbon, nor a single compound, but comprises a range of substances, the nature of which are heavily influenced by production conditions and fuel materials (Antal and Gronli, 2003). It is apparent that, along with highly stable, graphite-like polyaromatic 'organized' domains, charcoal can contain a variety of other carbon-based chemical structures (Pastorova et al., 1994; Baldock and Smernik, 2002; Ascough et al., 2008b). These comprise a complex disorganized phase containing aliphatic and aromatic moieties. This 'disorganized' phase appears to be more susceptible to diagenetic alteration than the organized phase (Cohen-Ofri et al., 2006). The presence of both organized and disorganized phases is also a feature of ancient archaeological charcoal samples (Cohen-Ofri et al., 2006) and is significant because different charcoal samples display variable resistance to environmental diagenesis. For example, charcoal carbon degradation has been observed on the order of decades in a Zimbabwean savannah soil (Bird et al., 1999) and virtually complete loss of charcoal due to fluctuating groundwater levels is recorded at an Australian archaeological site (Bird et al., 2002). However both the diagenetic processes affecting charcoal and the factors that determine the susceptibility of charcoal to these processes remain poorly understood.

Temperature-dependant chemical changes directly dictate the elemental and isotopic composition, physical appearance, and chemical structure of charcoal (Antal et al., 2003; Kim and Hanna 2006; McParland et al., 2007; Hall et al., 2008). These factors are likely to strongly influence post-depositional behaviour. Therefore reconstruction of charcoal production temperatures is of great interest. Possible production temperatures vary considerably, with 300-600°C being typical of natural fires (e.g. Swift et al., 1993). Data from natural wildfires suggests a range of <400°C to 800°C (Stinson and Wright, 1969, Stronach and McNaughton, 1989), while estimated production temperatures for charcoal in Roman hypocaust furnaces is 330-410°C (McParland et al., 2009a). Traditional methods of anthropogenic charcoal production have a range of 300-800°C (McParland et al. 2009b), while industrial processes such as pottery firing tend to involve higher temperatures up to and over 800°C (Livingstone-Smith 2001). Approaches to reconstruct production temperature include analysis of isotopic signatures and elemental compositional changes induced during heating (e.g. Werts and Jahren, 2007; Braadbart and Poole, 2008). However complicating factors must be considered, including species-specific carbon isotopic responses to pyrolysis and chemical exchange during post-depositional diagenesis (e.g. Bird et al., 2002; Turney et al., 2006; Ascough et al., 2008b).

An alternative approach to determining charcoal formation temperature is mean random reflectance (Ro_{mean}), derived from photometric measurement of the fraction of incident light radiation reflected from a sample surface under oil. Ro_{mean} is shown to have a positive relationship with formation temperature (Jones et al., 1991; Scott and Glasspool, 2005, 2007; McParland et al., 2007, 2009b), and is suitable for analysis of both ancient and freshly-produced charcoal samples (Jones et al., 1991; Scott and Jones, 1994; McParland et al., 2007, 2009a; Braadbart and Poole, 2008; Hudspith et al., 2010). Evidence from coal macerals indicates Ro_{mean} values increase with the fraction of aromatic carbon within a sample (Stach et al., 1982), meaning Ro_{mean} measurements may also provide valuable information on the chemistry of charcoal samples.

To assess the use of Ro_{mean} measurements in charcoal analysis requires consideration of a number of factors; in particular the potential effects of diagenetic alteration on

Ro_{mean} measurements. To achieve this, several different methods can be used, providing information on different aspects of samples. Such an approach is necessary because of initial heterogeneity in the chemical compounds present in different charcoal samples, and the additional variation introduced by diagenetic alteration. Here, we present the results of such a study, using a suite of modern analogue, natural and archaeological charcoal samples, where Ro_{mean} measurements are used in conjunction with a variety of other characterization techniques. H/C ratio is used to assess pyrolysis efficiency, while O/C ratio provides a measure of the degree of oxidation of a sample (Nguyen et al., 2004; Schmidt et al., 2001). Raman spectroscopy enables an estimation of the size and content of aromatic domains in carbonaceous materials (Tunistra and Konig, 1970), and the level of sample thermal reactivity can be established via thermogravimetric analysis (TGA) (Sima-Ella et al., 2005). In this way, the interplay between charcoal production mechanisms and the subsequent potential for post-depositional alteration is addressed.

Methodology

Charcoal samples

The first sample set (Table 1), comprised freshly-produced laboratory analogue charcoal (fresh charcoal = Fr_{char}) from two species. These were a low-density (0.41 ± 0.05 g/m^3) gymnosperm (Scots pine (*Pinus sylvestris L.*), Tentsmuir Forest, Fife), and a high density (0.88 ± 0.03 g/m^3) angiosperm, (mangrove (*Rhizophora apiculata* Blume), northeast Palawan, Philippines). Bark was removed and the wood processed by cutting into 1cm^3 cubes before conversion to charcoal in a controlled-atmosphere rotary furnace (Carbolite ™). The furnace was continuously purged with nitrogen at a constant metered flow rate of 7.0 l/min^{-1} and ramped at 10°C min^{-1} from room temperature to four final temperatures between 300-600°C, representing a typical range to which wood is heated in natural fires (e.g. Swift et al., 1993) and over which major chemical changes are known to occur (Williams and Besler, 1996). Temperature was monitored via a thermocouple inserted into a cube of wood in the furnace and the final temperature was held for 60 minutes, after which samples were cooled to room temperature under N_2. An aliquot of each charcoal was retained for reflectance measurement. Charcoal was ground to <500µm and treated with 0.5M HCl

153 to remove calcitic ash before neutralization and wet-sieving to 63-500μm followed by
154 drying at 40°C overnight. Analogue charcoal sample codes (Table 1) relate to the
155 wood species (P = Pine (*Pinus sylvestris*); M = Mangrove (*Rhizophora apiculata*))
156 and temperature of formation (300 to 600°C).
157
158 The second sample set comprised environmental charcoal (Env_{char}) samples (Env-1 to
159 Env-6), from six archaeological/palaeoenvironmental deposits of various ages,
160 obtained via consultation with specialists involved in site excavation or
161 archaeobotanical analysis (Table 1). Visible mineral material was removed from the
162 charcoal via sonication with deionized H_2O for 24 hours. A single, large charcoal
163 fragment was selected from each deposit for processing and split into two aliquots.
164 One aliquot was treated identically to the modern analogue samples (i.e. HCl followed
165 by wet-sieving to 63-500μm). The other aliquot was retained for measurement of
166 sample reflectance.
167
168 Env-1 was sampled from trees charred *in situ* within paroxysmal flow deposits of the
169 Maninjau caldera, west-central Sumatra (53400 ± 1400 ^{14}C yrs BP (Alloway et al.,
170 2004)), consisting of crudely stratified pumiceous lapilli and ash, overlain by andisol
171 and basaltic-andesite lapilli layers (Alloway et al., 2004). Env-2 was recovered from
172 a concentration of undated charcoal fragments within a lahar deposit developed from
173 basaltic eruptions from scoria cones spread along eruptive fissures at Praia do Norte,
174 northwest Faial Island, Azores (F. Tempera, pers comm.; Cruz et al., 2006).
175
176 Env-3 and Env-4 were recovered from the basal fill of Icelandic Norse-period
177 charcoal production pits. Env-3 was obtained in southern Iceland at Langanes,
178 previously dated to between 935 ± 35 and 960 ± 35 ^{14}C yrs BP, while Env-4 was
179 obtained from deposits close to Höskulsstaðir, Mývatnsveit, previously dated to 895 ±
180 35 BP (Church et al., 2007). In both cases, following final use of the pit, the basal fill
181 was covered with disturbed soil and turf, followed by ~500 years of natural soil
182 accumulation (Church et al., 2007).
183
184 Env-5 was recovered from a pile of charred wood within a house structure dated to ca.
185 1050 AD at Oursi-hubeero, a settlement site in the Sahel region of Burkina Faso

(Hallier and Petit, 2000; 2001). The deposits containing the charcoal were covered by sandy soils with clay inclusions derived from degradation of the mud brick structure (Hohn, 2005, Hohn pers comm). Finally, Env-6 was located in fluvial deposits of red sand and clay at Toca do Serrote da Bastiana, a rock shelter containing calcite deposits, in a Precambrian limestone outcrop in northeast Brazil (Steelman et al., 2002). The charcoal was recovered from a discontinuous layer at a depth of >50cm, overlying several burials dated to between 200 and 150 years BP (Guidon, N., pers comm).

Reflectance measurements

Individual charcoal fragments were embedded in resin and polished, then studied (using standard techniques for coal petrography) under a Nikon microphot microscope attached to Leica QWin image analysis software (Leica Image systems Ltd., 1997). Reflectance was measured under Cargill immersion oil (refractive index of 1.518 at 23^{o}C) using the x40 objective lens, illuminated with a 546nm light source. The instrument was calibrated against five standards (Spinel (Ro_{mean} 0.393), yttrium-aluminium garnet (Ro_{mean} 0.929), gadolinium-gallium garnet (Ro_{mean} 1.7486), cubic zirconium (Ro_{mean} 3.188) and silicon carbide (Ro_{mean} 7.506)). Reflectance measurements were made at 100 points per sample in order to calculate Ro_{mean} and standard deviation (SD) of Ro_{mean}.

Dichromate oxidation and SEM/TEM

Fr_{char} was digested via a modified Walkley-Black method in acidified potassium dichromate ($K_2Cr_2O_7$) (Bird and Gröcke, 1997). This methodology is commonly used in separation of fractions within carbonized biomass, where non-aromatic material, (e.g. cellulose), is preferentially removed (Wolbach and Anders, 1989; Bird and Gröcke, 1997). Briefly, cubes of charcoal were placed in 0.1M $K_2Cr_2O_7$ / 2M H_2SO_4 solution at 60°C in an incubator shaker for 72 hours. For the 300°C analogue charcoal this time period resulted in complete breakdown and dissolution, and a reduced oxidation period of 24 hours was used. After oxidation samples were neutralized by washing with deionized water and freeze-dried. Oxidative weight losses were recorded with a precision of ± 3%, based upon replicate analyses.

Oxidized charcoal samples were examined and split open to characterize any visual differences following oxidation. Where any visible alteration was observed, light microscopy and Transmission Electron Microscopy (TEM) analyses were performed. Specimens for TEM were embedded in Spurr Resin prior to sectioning by ultramicrotome. The ultra-thin sections, cut with a diamond knife, and not stained, were imaged with a Hitachi H7600 transmission electron microscope (TEM).

Elemental analysis

Carbon abundance (wt %) was measured in a Costech elemental analyser (EA) with a zero-blank auto-sampler, while oxygen and hydrogen abundance (wt %) was determined using high-temperature flash pyrolysis in a ThermoFinnigan High-Temperature Conversion Elemental Analyzer (TC/EA). Samples were measured in duplicate with laboratory standards and blanks. Both the EA and TC/EA were coupled through a ThermoFinnigan ConFlo III to a ThermoFinnigan Delta XL Plus mass spectrometer. Elemental abundances were calculated using comparison of gas pulse peak area and mass to that of acetanilide (IAEA/Sigma Aldrich, %C: 71.09%, %O: 11.84%, %H: 6.71%), where the external reproducibility was better than 0.5%, 0.7% and 0.4% for C, O and H, respectively.

Raman spectroscopy

Raman spectroscopic measurements were made of Fr_{char} prepared at 300°C and 600°C, and of Env_{char} samples that gave high (Env-1 and Env-2) and low (Env-5 and Env-6) Ro_{mean} values. A compacted pellet of powdered charcoal was produced from each individual sample prior to analysis. Measurements were made at the Weizmann Institute of Science, Israel, in air at room temperature using a Renishaw 2000 Raman Imaging Microscope through a 50X lens without a polarizer. The excitation at 632 nm was produced by a 25mw HeNe laser. Each measurement was made 8 times at random locations on each charcoal pellet, and the maximum peak height and peak position were determined and averaged.

TGA

254

255 Thermogravimetric analysis (TGA) was performed on the analogue charcoal prepared
256 at 300°C and 600°C and on environmental charcoal using a 'Thermal Analysis' SDT
257 Q600 TGA/DSC. Samples were heated at 50°C min^{-1} to 525°C under nitrogen to
258 facilitate removal of volatiles, and mass loss due to volatile decomposition was
259 calculated. Upon reaching 525°C, the samples were isothermally combusted in air for
260 20 minutes and carbon burnout profiles generated. Two quantitative measures of
261 reactivity were then taken; firstly a time until 90% carbon conversion and, secondly,
262 pseudo-first order kinetics were applied, between 5 and 95% carbon burnout, to allow
263 the calculation of a composite rate constant via:

264 $$\frac{\partial \alpha}{\partial t} = k(1-\alpha) \qquad (1)$$

265 Where $\alpha = (1\text{-}C/C_0)$ is the fractional weight conversion, C is the remaining carbon
266 mass and C_0 is the original carbon mass (Sima-Ella, et al., 2005).
267

268 **Results**
269

270 *Reflectance*
271

272 Ro_{mean} values for Fr_{char} range between 0.03 ± 0.01 for M-300 to 4.01 ± 0.52 for M-600
273 (Table 2), and are within the range of previous studies (Scott, 1989; Jones et al., 1991;
274 Guo and Bustin, 1998). Although mangrove charcoal Ro_{mean} is slightly higher than
275 pine at 500-600°C, Ro_{mean} from both species is consistently within analytical error,
276 and is strongly correlated ($r^2 = 0.99$, $P < 0.05$) with production temperature (Figure 1)
277 following the polynomial function:
278

279 $$y = 1E\text{-}0.5x^2 + 0.0011\text{-}1.2855 \qquad (2)$$
280

281 Production temperatures calculated for Fr_{char} using this calibration accurately reflect
282 the known temperature to ± 15°C. Calculated production temperatures for Env_{char} via
283 the calibration are 516 ± 33°C for Env-1 (Ro_{mean} = 2.51 ± 0.45) and 497 ± 25°C for
284 Env-6 (Ro_{mean} = 2.26 ± 0.33). For Env-3, Env-4 and Env-5, a temperature range of
285 351 ± 23°C to 361 ± 25°C is obtained, while the lowest production temperature, 320 ±
286 29°C, is calculated for Env-2. We note, however that reflectance increases slightly

with time for up to 24 hours (Scott and Glasspool, 2005; McParland et al., 2009b) meaning charring experiments of longer durations are needed to provide precise formation temperatures. However, comparisons of reflectance and temperature derived from the one hour curves do appear to approximate to known and inferred temperatures from studies of wildfire charcoals (Scott and Jones, 1994; Scott et al., 2000).

Dichromate oxidation

The Ro_{mean} of Fr_{char} produced at 400°C and above is not significantly different after oxidation for either species (Table 2). Observable changes in mass after $K_2Cr_2O_7$ oxidations were only recorded in P-300 and M-300 (Table 2), with respective mass loss of 73% and 36%. High loss rates and physical sample breakdown during oxidation meant reliable recovery of sufficient material for reflectance measurement was not possible from P-300 and M-300. After oxidation, visible alteration was only apparent in P-300, consisting of a lightening in colour of the outer sample surface. Light microscopy (Figure 2) revealed these colour changes were limited to the outer few sample cells, and provided no strong evidence for structural alteration. Although TEM analysis of cell walls in the region of colour change showed slight evidence for thinning, this was of very limited extent (Figure 3). The mass loss in 300°C charcoals is therefore likely to relate to the removal of chemical compounds, without major alteration of the charcoal physical structure.

Elemental analysis

Carbon content of Fr_{char} showed a strong, non-linear dependence on temperature (Table 3). Carbonized materials fall into discreet regions on two-dimensional van Krevelen diagrams depending upon their elemental content (van Krevelen, 1950; Hockaday et al., 2007), and a diagram of the Fr_{char} shows linear decrease in O/C and H/C ratios with temperature. Atomic ratios are highly similar between species at ≥400°C (Figure 4). However, there is an offset in H and O content between pine and mangrove that is most apparent at 300°C, where mangrove charcoal contains significantly less of these elements and hence appears more efficiently charred.

Using the Ro_{mean}-based production temperature, the atomic ratios for each Env_{char} were compared with those of Fr_{char} for an equivalent production temperature. For Env-1, the O/C and H/C ratios are consistent with those of equivalent Fr_{char}. However in the remainder of Env_{char} the atomic ratios differ from that of equivalent Fr_{char}. In Env-2 and Env-5 both H/C and O/C ratios are higher than equivalent (i.e. ~320-350°C) analogue samples. In Env-3 and Env-4 the O/C atomic ratio is consistent with ~300°C analogue samples, meaning the O/C atomic ratio is slightly higher than expected. For these samples the H/C ratios are lower than that predicted for this temperature from the Ro data, being more similar to the analogue charcoals produced at ~450°C. In Env-6 although the H/C atomic ratio is consistent with those of equivalent (i.e. ~500°C) analogue charcoal, the O/C atomic ratio is more similar to that of analogue charcoal produced at ~300°C (Figure 2). It may be noted that comparisons are broad as the exact charring times of the environmental charcoal samples are not known.

Raman spectroscopy

Raman spectroscopy provides information on the molecular structure and chemical bonding of carbon atoms. The Raman spectra of graphitic carbon contains a band at 1575 cm^{-1} (the G band), assigned to in-plane stretching motions of carbon sp^2 atoms (Tuinstra and Koenig, 1970), representing highly stable, ordered carbon configurations. A second band at 1350 cm^{-1} (the D band) represents disordered carbon configurations, arising from defects and discontinuities in crystallites, and has been assigned to carbons with an sp^3 configuration, not located in graphitic layers, likely to be tetrahedrally bonded (Tuinstra and Koenig, 1970; Dresselhaus et al., 2000; Fey and Kao, 2002; Fung et al., 1993). Samples with narrower G bands, positioned closer to 1575 cm^{-1} contain increasing area and amount of ordered, microcrystallite domains (Tunistra and Konig, 1969; Knight and White, 1989).

Raman peaks in spectra of P-600 and M-600 are more highly resolved, suggesting greater chemical homogeneity compared P-300 and M-300 (Table 4). The presence of a G peak indicates some organized graphitic microcrystallites are present in both 300°C and 600°C charcoal, however the narrower G peaks at lower frequencies (1584 cm^{-1}) suggests a more highly ordered carbon structure in P-600 and M-600. The G peak positions also suggest a slightly higher proportion of ordered carbon in

mangrove charcoal. The position of the D peaks is not conclusively different between the samples, however these are considerably broader in the 300°C charcoals.

The presence of a G peak also indicates a proportion of organized carbon domains within the Env_{char}. Samples Env-1 and Env-6 closely resemble the 600°C Fr_{char}, with narrow G peaks at 1584 cm^{-1}. In contrast, the Raman spectra of Env-5 and Env-2 more closely resemble the 300°C analogue samples, with broad G peaks centred at 1590-1600 cm^{-1} (Table 4). In these samples, the D peaks are also broader and positioned at a higher frequency than that of Env-1 and Env-5. Overall, the degree of structural order in the analogue and environmental samples can be broadly related to Ro_{mean}, with higher Ro_{mean} in samples showing narrow G peaks at a lower frequency (Figure 5).

TGA

Sample reactivity during TGA relates to the thermal resistance of its molecular content. The bond energies of individual aromatic rings are ~193.71 Kcal mol^{-1}, and can be much higher as the size of polyaromatic structures increases (Maitland et al., 2005). Bond energies in non-aromatic components, such as C-C (80.711 Kcal mol^{-1}) and C-H (92.241 Kcal mol^{-1}), can be much lower, and these are broken at an earlier stage in TGA. Following devolatilization, the time taken for sample burnout increases proportionally to chemical stability. Charcoal with a higher proportion of non-aromatic structures has lower thermal stability, and is therefore expected to show i.) higher mass loss during devolatilization, and ii.) decreased burnout times and composite first order rate constants.

In Fr_{char} the reactivity of pine charcoal is clearly higher than that of mangrove for both 300°C and 600°C charcoals (Table 5), with similar time to 90% burnout in both M-300 and P-600 (7.4 versus 7.3 minutes, respectively). In both species there is a large difference in volatile content between 300°C and 600°C charcoal, with ~30-50% low thermal stability material in P-300 and M-300, compared to ~6% volatiles in P-600 and M-600, indicating much higher content of non-aromatic compounds in the 300°C charcoal.

In Env_{char}, Env-1 and Env-6 show high thermal stability, with burnout times and first order rate constants similar to M-600. Volatile content in Env-1 is comparable to the 600°C analogue samples, however Env-6 contains ~20% volatile material. The remaining four Env_{char} samples are more reactive, generally intermediate between P-300 and P-600. In this group, Env-3 is the most thermally stable, and Env-4 the least, and it appears that these samples contain a relatively high proportion of material in a chemical form that is more susceptible to thermal degradation.

Discussion

Analogue charcoal: Relationship between production temperature, chemical characteristics and Ro_{mean}

The results clearly demonstrate the strong relationship between production temperature and chemical characteristics in charcoal. At higher production temperatures, O/C and H/C ratios of Fr_{char} fall. This is due to progressive dehydrogenation and deoxygenation reactions as polycondensed aromatic structures are formed and polyaromatization (i.e. growth in the size of the aromatic sheets) becomes dominant (Nishimiya et al., 1998; Trompowsky et al., 2005). Fr_{char} produced at lower temperatures is heterogeneous, containing higher proportions of oxygen, hydrogen, and disorganized carbon, evidently derived from incomplete thermal decomposition of lignocellulosic material (e.g. Baldock and Smernick, 2002; Ascough et al., 2008b). The extent of organized carbon microcrystallites is smaller in Fr_{char} produced at lower temperatures, presumably meaning a less well-developed aromatic structure exists in these samples.

Differences in the extent of organized carbon microcrystallite domains and thermal stability are apparent between the two analogue species, with less highly ordered carbon structures in pine charcoal than in mangrove charcoal formed at the same temperature. These may relate to variations in the proportion of chemically different components in the starting wood (e.g. Ascough et al., 2008b), resulting in less complete thermal degradation and aromatization of initial wood macromolecules in pine. This interpretation is supported by differences in the elemental composition of

422 the 300°C charcoal, where pine charcoal is closer to the composition of the un-
423 pyrolysed wood, containing a relatively high proportion of oxygen and carbon.
424
425 The strong linear correlation between Ro_{mean} and content of carbon microcrystallites
426 supports the interpretation that Ro_{mean} is a function of the amount of ordered, aromatic
427 carbon in a sample, which in turn is predominantly a function of temperature. Despite
428 the differences in species described above, the Ro_{mean} values for both species are
429 within analytical uncertainty at equivalent temperatures, suggesting that species-
430 dependant chemical differences are insufficient to result in a significant Ro_{mean} offset.
431
432 Ro-based temperatures calculated in this study are consistent with previous work,
433 where Ro_{mean} values >2.0 were only observed above 400°C, regardless of heating
434 duration (Guo and Bustin, 1998; McParland et al., 2009b). An important point is that
435 after exposure of biomass to temperatures much lower than 300°C, Ro_{mean} is likely to
436 be extremely low and therefore increasingly difficult to quantify as cell wall outlines
437 become increasingly difficult to image in reflected light. However, the clear
438 relationship between Ro_{mean} and production temperature in the range tested here
439 demonstrates the power of the technique to accurately reconstruct production
440 temperatures for wood charcoal produced at 300-600°C, an interpretation supported
441 by other work in this field (e.g. Hudspith et al., 2010). It is also evident that in
442 samples produced at ≥400°C, Ro_{mean} values are not altered by the $K_2Cr_2O_7$ treatment,
443 indicating that the organized domains are not significantly oxidized during the
444 treatment. This means that even following exposure to conditions of extreme
445 degradation potential, reflectance measurements appear to still be a robust measure of
446 production temperature in these samples. Therefore, where Ro_{mean} measurements of
447 environmental samples indicate production above 400°C, and the sample appears
448 structurally intact, the values of an assemblage as a whole are less likely to have been
449 influenced by diagenetic processes. It is theoretically conceivable that such processes
450 could affect Ro_{mean} if the result was a large-scale breakdown of charcoal aromatic
451 structure, reducing the size of polyaromatic domains throughout the entire sample, but
452 we have no evidence of this. As it is not possible to use Ro_{mean} measurements to
453 assess potential post-depositional alteration of charcoal assemblages, alternative
454 analytical methods are required to achieve this, as part of an integrated approach.

In the 300°C samples, where material does survive the $K_2Cr_2O_7$ treatment, it appears not to have undergone major structural alteration at the macroscopic to cellular level (Figures 2 and 3). This suggests that although a significant proportion of the 300°C charcoal is readily oxidizable, these charcoals also contain a resistant component. It is possible that this aromatic component is more highly degradable as a result of the smaller microcrystallite extent in low temperature Fr_{char}, as atoms at the edge of polyaromatic domains are more reactive than those within layer planes, meaning that oxidation occurs preferentially at edge and defect sites (Walker et al., 1959; Boehm et al., 1994). The mass loss during the $K_2Cr_2O_7$ treatment in 300°C Fr_{char} suggests that a significant proportion of the structure of low temperature charcoal is likely to be comprised of a disorganized phase, which is quite readily susceptible to oxidative degradation. If such degradation had the potential to alter the measured Ro_{mean} of low temperature charcoal, this could affect interpretative accuracy based upon measurements of affected material. However it should be stressed that the evidence does not show that this is so. Until now reflectance measurements of charcoals giving temperatures between 300 and 400^{o}C appear to give consistent and reliable results (see below). However, the concept that lower temperature charcoal samples are subject to greater diagenetic degradation has implications that should be considered. If a temperature is derived from Ro_{mean} measurements of a suite of charcoal particles that have been subject to significant oxidation, then a higher overall temperature may be inferred that is the actual average for the particle group. This would be due to more rapid degradation of the lower temperature charcoals, leaving only the charcoals formed at higher temperatures. Therefore, it is important that where Ro_{mean} measurements indicate productions temperatures < 400^{o}C, the potential for diagenetic alterations of the sample be carefully assessed, for the reasons highlighted above. If such alteration is suspected, the methodological approaches employed in this study (e.g. elemental analysis) appear well suited as diagnostic tools, as demonstrated from the environmental charcoal samples.

Environmental charcoal: reconstruction of production temperature and evidence for diagenetic alteration

488 It should be noted that, unlike the experimentally produced charcoal where a charring
489 time is known, in our environmental charcoals this is not so. This means, therefore,
490 that the interpreted charring temperatures represent minimum charring temperatures
491 and only where the time may be indicated from the nature of the deposit (e.g. in hot
492 pyroclastic flows, charcoal clamps) can an exact temperature be calculated (see
493 McParland et al., 2009b for discussion).
494
495 Env-1 appears to be a high temperature (>500°C) charcoal that has not been subject to
496 alteration during deposition, as the sample elemental composition, ordered carbon
497 content, volatile content and reactivity are all consistent with those of equivalent
498 analogue charcoal. Although Env-1 is of considerable antiquity (>50 Ka BP (Alloway
499 et al., 2001, Ascough et al., 2008a), the conditions of burial indicate slow soil
500 formation processes and a lack of well-defined soil horizons (Alloway et al., 2001). It
501 is possible that this resulted in exposure of Env-1 to a low range of degradation
502 processes, contributing to the apparently pristine nature of this charcoal. The
503 characteristics of this sample support previous interpretations that charcoal-derived
504 black carbon can show extreme resistance to environmental degradation over very
505 extended time periods (e.g. Liang et al., 2008).
506
507 In the case of Env-6, the Ro_{mean} temperature assessments (497 ± 25°C) are consistent
508 with pyrolysis efficiency estimated by H/C ratio, content of organized carbon and
509 reactivity. However, this charcoal contains a larger amount of low thermal-stability
510 volatile material and higher oxygen content than that predicted from analogue
511 charcoal for this temperature. This suggests Env-6 may be affected by diagenetic
512 alteration resulting in the addition of oxygen to the charcoal chemical structure.
513 Previous observations suggest that carboxylation processes play an important role in
514 charcoal diagenesis (e.g. Cohen-Ofri et al., 2006) and the addition of –COOH groups
515 would explain the increased oxygen content in Env-6. However, all other analysis
516 results support the results of Ro_{mean} measurements, suggesting that the processes
517 affecting elemental composition have not affected the accuracy of the Ro-based
518 temperature reconstruction for this sample.
519

520 The Ro_{mean} data suggests Env-3 and Env-4 were produced at 361 ± 24°C and 351 ±
521 41°C, respectively. These samples have similar atomic ratios and volatile content, and
522 TGA data shows higher reactivity in Env-4, which would be consistent with
523 production at a slightly lower temperature. All data are consistent with results of
524 analogue charcoal, apart from the atomic ratios. The slightly higher than predicted
525 O/C ratio indicates the possibility that oxygen has been added to the charcoal
526 structure. However, in these samples the H/C ratios are also significantly lower than
527 predicted for charcoal produced at ~350°C. In this instance, diagenetic alteration may
528 have involved dehydrogenation reactions, resulting in the loss of CH_2 and CH_3 groups
529 from aliphatic molecules that were incompletely converted to aromatic compounds
530 below 400°C. In the final two environmental samples, Env-2 and Env-5, Ro_{mean}
531 measurements again suggest production at <400°C. Both the oxygen and hydrogen
532 content of these samples is somewhat higher than that predicted from equivalent
533 analogue charcoal, again suggesting that some diagenetic alteration has occurred. In
534 such samples, it is important to consider the possibility that this material represents
535 the highly degraded remains of an initially more pristine charcoal structure. However,
536 the organized carbon content, reactivities, and volatile content (34.10% and 41.13% of
537 dry, ash-free sample weight) of these charcoals are all comparable to that of the
538 300°C analogue charcoal, supporting the reliability of the Ro_{mean} temperature
539 assessments. An additional consideration is that in these samples the non-aromatic
540 component may represent incompletely converted, and possibly diagenetically altered,
541 lignocellulosic components of the original plant material, or material derived from
542 exogeneous sources to the original plant, such as soil humic acids. In comparison to
543 charcoal, these materials contain a relatively high proportion of oxygen and hydrogen,
544 that may contribute to the observed O/C and H/C ratios in Env-2 and Env-5.
545
546 *Implications for archaeological and palaeoenvironmental investigation*
547
548 The concept of a continuum in degradation potential has important implications for
549 the use of charcoal within archaeological research. For example, diagenetic processes
550 can affect radiocarbon dating accuracy; at the early human occupation site of
551 Nauwalabila, post-depositional alteration of some charcoal was so severe that samples
552 did not reliably reflect the sediment deposition date (Bird, et al., 2002). Additionally,

553 loss or alteration of charcoal following deposition may significantly affect the
554 accuracy of quantitative estimates of fire histories. The issue is greatly complicated by
555 the range in conditions of charcoal production that are likely to exist in most
556 instances, from settings such as domestic hearths to forest wildfires. Here, a gradient
557 in production temperature has the potential to produce charcoal with different
558 chemical characteristics that enters the depositional record at a single point in time.
559 The data also appear to indicate that deposition conditions play a key role in charcoal
560 alteration, as ancient samples such as Env-1 may show less apparent alteration than
561 younger samples exposed to a different set of environmental conditions, but which
562 were initially exposed to a comparable temperature range (e.g. Env-6).
563
564 The results presented here highlight the value of integrating Ro_{mean} with other
565 analytical methods in charcoal analysis when assessing the likely diagenetic alteration
566 of charcoal assemblages. Useful approaches in this regard are elemental analysis,
567 Raman spectroscopy and TGA. These methods require small sample quantities (on the
568 order of mg), are rapid and relatively low-cost. Pyrolysis efficiency and the degree of
569 charcoal oxidation is provided by H/C and O/C ratio, respectively, while the extent of
570 aromatic domains in the charcoal, and its chemical resistance can be assessed via
571 Raman spectroscopy and TGA. In particular, it appears that addition of oxygen to the
572 charcoal chemical structure may occur during exposure to environmental conditions,
573 as suggested previously (e.g. Cohen-Ofri et al., 2006). Therefore an approach
574 integrating these methods allows assessment of the potential for post-depositional
575 alteration, particularly where charcoal samples may have been produced at lower
576 temperature. Where Ro_{mean} measurements suggest production under 400°C, this
577 indicates that the charcoal sample contains a variety of chemical compounds other
578 than polyaromatic carbon. These could represent remains of incomplete conversion of
579 plant macromolecules, degradation of the charcoal aromatic structure, or sources of
580 exogenous contamination.
581
582 Important added value is provided from investigation integrating several
583 methodological approaches as a means of evaluating deliberate production of specific
584 charcoal types. For example, it is interesting to note that although Env-3 and Env-4
585 were produced in different locations, the charcoal is chemically very similar. This
586 suggests a consistency in production methodology and charcoal quality between the

two sites, and the possibility that this represented optimization of charcoal quality at a particular site with regard for its intended purpose, an interpretation that is consistent with archaeological data for this region (e.g. Church et al., 2007).

Conclusions

The present study further emphasises that mean random reflectance under oil (Ro_{mean}) of a charcoal sample is strongly positively correlated with the sample production temperature. As Ro_{mean} measurements are applicable for analysis of both ancient and freshly-produced charcoal samples, the technique has important benefits for archaeological and palaeoenvironmental investigations, as it provides quantitative information on fire regime in both natural (e.g. wildfire) and anthropogenic (e.g. domestic hearth) settings. In this study we use an integrated methodological approach (i.e. Ro_{mean} coupled with elemental analysis, Raman spectroscopy and TGA) to show that Ro_{mean} is also strongly correlated with the extent of organized, polyaromatic domains within charcoal. Along with reliable temperature reconstructions, Ro_{mean} therefore also provides information on the chemical structure of charcoal. This chemical structure is clearly strongly dependant upon production temperature, and the results show that charcoal produced at lower temperatures (e.g. 300°C) displays both higher reactivity and chemical heterogeneity. As diagenetic processes can potentially alter lower temperature (<400°C) charcoals, there may be a need to assess the level of diagenetic alteration with other methods for charcoal characterization. The results presented here highlight an overall continuum in charcoal 'degradability' that is dependant upon fuel material and production conditions. Diagenetic alteration and loss of material appears more likely if initial charcoal production temperatures were <400°C. This has importance for the use of charcoal as an archaeological and palaeoenvironmental proxy data source. For example, post-depositional loss of charcoal could affect interpretations of fire histories that are based upon variations in charcoal abundance. The concept of diagenetic alteration also has implications for wider applications, including the use of 'biochar' charcoal as a long-term carbon sequestration tool.

Acknowledgements

Funding for this research was provided by NERC standard grant NE/C004531/1 'Charcoal Degradation in Natural Environments'. This research represents a contribution from SAGES (The Scottish Alliance for Geosciences, Environment and Society). The authors gratefully acknowledge the assistance of Steve Weiner and the staff of the Kimmel Centre for Archaeological Science at the Weizmann Institute, Israel. Environmental charcoal samples were made available for analysis with the kind assistance of Brent Alloway, Alexandra Hohn, Antonio Valera, Neide Guidon and Mike Church. We would like to thank Tony Brain (CUI, Kings College London) for technical assistance with the TEM work and Sharon Gibbons and Neil Holloway (RHUL) for help with sample preparation for reflectance microscopy.

629 References

630

631 Alloway, B. V., Pribadi, A., Westgate, J. A., Bird, M., Fifield, L. K., Hogg, A., Smith
632 I., 2004. Correspondence between glass-FT and AMS 14 C ages of silicic pyroclastic
633 density current (PDC) deposits sourced from Maninjau caldera, west-central Sumatra.
634 Earth and Planetary Science Letters 227, 121-133.

635

636 Antal, M. J., Gronli, M. G., 2003. The Art, Science, and Technology of Charcoal
637 Production. Ind. Eng. Chem. Res. 42, 1619-1646.

638

639 Ascough P. L., Bird M. I., Brock F., Higham T. F. G., Meredith W., Snape C., Vane
640 C. H. 2008a. Hydropyrolysis as a new tool for radiocarbon pretreatment and the
641 quantification of black carbon. Quaternary Geochronology 4 (2), 140-147.

642

643 Ascough, P., Bird, M. I., Wormald, P., Snape, C. E., Apperley, D., 2008b. Influence
644 of pyrolysis variables and starting material on charcoal stable isotopic and molecular
645 characteristics. Geochimica et Cosmochimica Acta 72, 6090-6102.

646

647 Baldock, J.A., Smernik, R. J., 2002. Chemical composition and bioavailability of
648 thermally altered Pinus resinosa (Red pine) wood, Organic Geochemistry 33, 1093–
649 1109.

650

651 Bird, M.I., 2006. Radiocarbon dating of charcoal. In: Elias, S.A. (Ed.) The
652 Encyclopaedia of Quaternary Science, Elsevier, Amsterdam, pp. 2950–2957.

653

654 Bird M.I., Gröcke D.R., 1997. Determination of the abundance and carbon isotope
655 composition of elemental carbon in sediments. Geochimica et Cosmochimica Acta 61,
656 3413–3423.

657

658 Bird, M. I., Moyo, E., Veenendaal, E., Lloyd, J. J., Frost, P., 1999. Stability of
659 elemental carbon in a savanna soil. Global Biogeochemical Cycles 13, 923-932

660

661 Bird M. I., Turney, C. S. M., Fifield, L. K., Jones, R., Ayliffe, L. K., Palmer, A.,
662 Cresswell, R. G., Robertson, S., 2002. Radiocarbon analysis of the early

663 archaeological site of Nauwalabila 1, Arnhem Land, Australia: Implications for
664 sample suitability and stratigraphic integrity. Quaternary Science Reviews 21, 1061-
665 1075.
666
667 Boehm, H., Setton, R., Stumpp, E., 1994. Nomenclature and terminology of graphite
668 intercalation compounds (IUPAC Recommendations 1994). Pure Appl. Chem. 66,
669 1893.
670
671 Braadbaart, F., Poole, I., 2008. Morphological, chemical and physical changes during
672 charcoalification of wood and its relevance to archaeological contexts. Journal of
673 Archaeological Science 35, 2434-2445
674
675 Church, M. J., Dugmore, A. J., Mairs, K-A., Millard, A., Cook, G. T.,
676 Sveinbjarnardóttir, G., Ascough, P. A., Newton, A. J., Roucoux, K., 2007. Charcoal
677 production during the Norse and early medieval periods in Eyjafjallahreppur,
678 Southern Iceland. Radiocarbon 49, 659-672.
679
680 Cohen-Ofri, I., Weiner, L., Boaretto, E., Mintz, G., Weiner, S., 2006. Modern and
681 fossil charcoal: aspects of structure and diagenesis. Journal of Archaeological Science
682 33, 428-439
683
684 Collinson, M. E., Featherstone, C., Cripps, J. A., Nichols, G. J., Scott, A. C., 2000.
685 Charcoal-rich plant debris accumulations in the Lower Cretaceous of the Isle of
686 Wight, England. Acta Palaeobotanica 164, 93–105.
687
688 Cruz, J. V., Antunes, P., Amaral, C., Franca, Z., Nunes, J.C., 2006. Volcanic lakes of
689 the Azores archipelago (Portugal): Geological setting and geochemical
690 characterization. Journal of Volcanology and Geothermal Research 156, 135-157.
691
692 Darmstadt, H., Pantea, D., Summchen, L., Roland, U., Kaliaguine, S., Roy, C., 2000.
693 Surface and bulk chemistry of charcoal obtained by vacuum pyrolysis of bark:
694 influence of feedstock moisture content. Journal of Analytical and Applied Pyrolysis
695 53, 1-17.
696

697 Dresselhaus, M. S., Pimenta, M.A., Ekiund, P.C., Dresselhaus, G., 2000. Raman
698 Scattering in Fullerenes and Related Carbon-based materials. In: Weber W.H., Merlin,
699 R. (Ed.s) Raman Scattering in Materials Science. Springer, 2000
700
701 Eckmeier, E., Gerlach, R., Skjemstad, J. O., Ehrmann, O., Schmidt, M. W. I., 2007.
702 Only small changes in soil organic carbon and charcoal found one year after
703 experimental slash-and-burn in a temperate deciduous forest. Biogeosciences Discuss.
704 4, 595-614.
705
706 Fey, G. T. K., Kao, Y.C., 2002. Synthesis and characterization of pyrolyzed sugar
707 carbons under nitrogen or argon atmospheres as anode materials for lithium-ion
708 batteries. Materials Chemistry and Physics 73, 37-46.
709
710 Fung, A. W. P., Rao, A. M., Kuriyama, K., Dresselhaus, M. S., Dresselhaus, G.,
711 Endo, M., Shindo, N., 1993. Raman-Scattering and Electrical Conductivity in Highly
712 Disordered Activated Carbon-Fibers. Journal of Materials Research 8 , 489-500.
713
714 Gouveia, S. E. M., Pessenda, L. C. R., Aravena, R., Boulet, R., Scheel-Ybert, R.,
715 Bendassoli, J. A., Ribeiro, A. S., Freitas, H. A., 2002. Carbon isotopes in charcoal and
716 soils in studies of paleovegetation and climate changes during the late Pleistocene and
717 the Holocene in the southeast and centerwest regions of Brazil. Global and Platetary
718 Change 33, 95-106.
719
720 Guo, Y., Bustin, R. M., 1998. FTIR spectroscopy and reflectance of modern charcoals
721 and fungal decayed woods: implications for studies of inertinite in coals. International
722 Journal of Coal Geology 37, 29-53
723
724 Hall G., Woodborne, S., Scholes, M. 2008 Stable carbon isotope ratios from
725 archaeological charcoal as palaeoenvironmental indicators. Chemical Geology 247,
726 384-400.
727
728 Hallier, M., Petit, L. P., 2000 Tertres d'occupation et d'autre formes d'habitation à
729 l'âge de Fer : Rapport préliminaire de la campagne archéologique en été 2000 au nord
730 du Burkina Faso. Nyame Akuma 54, 2-5

731
732 Hallier, M., Petit, L. P., 2001 Fouille d'une maison de l'Age du Fer dans le nord du
733 Burkina Faso. Nyame Akuma 56, 2-3
734
735 Hockaday, W. C., Grannas, A. M., Kim, S., Hatcher, P. G., 2007. The transformation
736 and mobility of charcoal in a fire-impacted watershed, Geochimica et Cosmochimica
737 Acta 71, 3432-3445.
738
739 Höhn, A., 2005. Zur eisenzeitlichen Entwicklung der Kulturlandschaft im Sahel von
740 Burkina Faso. Untersuchungen von archäologischen Holzkohlen. Unpublished PhD
741 thesis, Universität in Frankfurt am Main.
742
743 Hudspith, V., Scott, A.C., Wilson, C. and Collinson, M.E., 2010. The preservation by
744 plants by volcanic processes: an example from the Taupo Ignimbrite, New Zealand.
745 Palaeogeography, Palaeoclimatology, Palaeoecology
746 doi:10.1016/j.palaeo.2009.06.036
747
748 Jones, T., Scott, A. C., Cope, M., 1991. Reflectance measurements against
749 temperature of formation for modern charcoals and their implications for the study of
750 fusain. Bull. Geol. Soc. France 162, 193-200.
751
752 Kim, N. H., Hanna, R. B., 2006. Morphological characteristics of Quercas variabilis
753 charcoal prepared at different temperatures. Wood Science and Technology 40, 392
754
755 Knight, D.S., White, W.B. 1989. Characterization of Diamond Films by Raman-
756 Spectroscopy. Journal of Materials Research 4, 385–393.
757
758 Levine, J. S., 1991. Global biomass burning: Atmospheric, climatic, and biospheric
759 implications. The MIT Press, Cambridge, Massachusetts.
760
761 Liang, B., Lehmann, J., Solomon, D., Sohi, S., Thies, J. E., Skjemstad, J. O., Luizao,
762 F. J., Engelhard, M. H., Neves, E. G., Wirick, S., 2008. Stability of biomass-derived
763 black carbon in soils, Geochimica et Cosmochimica Acta 72, 6069-6078.
764

765 Livingstone-Smith, A., 2001. Bonfire II: the return of pottery firing temperature.
766 Journal of Archaeological Science 28, 991–1003.
767
768 Maitland, J., 2005. Organic chemistry, New York, W.W. Norton
769
770 McParland, L., Collinson, M.E., Scott, A.C., Steart, D., 2007. Ferns and Fires:
771 Experimental charring of ferns compared to wood and implications for paleobiology,
772 coal petrology and isotope geochemistry. PALAIOS 22, 528-538.
773
774 McParland, L C., Hazell, Z., Campbell, G., Collinson, M. E., Scott, A. C., 2009a.
775 How the Romans got themselves into hot water: temperatures and fuel types used in
776 firing a hypocaust. Environmental Archaeology 14, 176-183.
777
778 McParland, L C., Scott, A. C., Collinson, M. E., Campbell, G., 2009b. The use of
779 reflectance values for the interpretation of natural and anthropogenic charcoal
780 assemblages. Archaeological and Anthropological Sciences. DOI 10.1007/s12520-
781 009-0018-z
782
783 Moore, J., 2000. Forest fire and human interaction in the early Holocene woodlands
784 of Britain.. Palaeogeography, Palaeoclimatology, Palaeoecology 164, 125–137.
785
786 Nguyen, T. H., Brown, R. A., Ball, W. P., 2004. An evaluation of thermal resistance
787 as a measure of black carbon content in diesel soot, wood char, and sediment. Organic
788 Geochemistry 35, 217-234.
789
790 Nishimiya, K., Hata, T., Imamura, Y., Ishihara, S. 1998 Analysis of chemical
791 structure of wood charcoal by X-ray photoelectron spectroscopy. Journal of Wood Sci
792 44, 56–61.
793
794 Pastorova, I., Botto, R. E., Arisz, P. W., Boon, J. J., 1994. Cellulose char structure: a
795 combined analytical Py-GC-MS, FTIR, and NMR study. Carbohydrate. Research 262,
796 27−47.
797

798 Pessenda, L. C. R., Aravena, R., Melfi, A. J., Telles, E. C. C., Boulet, R., Valencia, E.
799 P. E., Tomazello, M., 1996. The use of carbon isotopes (C-13, C-14) in soil to
800 evaluate vegetation changes during the Holocene in Central Brazil. Radiocarbon 38,
801 191-201.
802
803 Preston, C. M., Schmidt, M. W. I., 2006. Black (pyrogenic) carbon: a synthesis of
804 current knowledge and uncertainties with special consideration of boreal regions.
805 Biogeoscience 3, 397-420.
806
807 Scott, A.C., 1989. Observations on the nature and origin of fusain. International
808 Journal of Coal Geology. 12, 443-475
809
810 Scott, A.C. 2000. The Pre-Quaternary History of Fire. Palaeogeography,
811 Palaeoclimatology, Palaeoecology, 164, 281-329
812
813 Scott, A.C., 2009. Forest Fire in the Fossil Record. pp. 1-37. In: Cerdà, A.,
814 Robichaud, P. (eds). Fire Effects on Soils and Restoration Strategies. Science
815 Publishers Inc. New Hampshire.
816
817 Scott, A.C., 2010. Charcoal recognition, taphonomy and uses in palaeoenvironmental
818 analysis. Palaeogeography, Palaeoclimatology, Palaeoecology.
819 doi:10.1016/j.palaeo.2009.12.012.
820
821 Scott, A.C., Glasspool, I.J., 2005. Charcoal reflectance as a proxy for the
822 emplacement temperature of pyroclastic flow deposits. Geology 33, 589-592.
823
824 Scott, A.C., Glasspool, I.J., 2007. Observations and Experiments on the Origin and
825 Formation of Inertinite Group Macerals. International Journal of Coal Geology 70,
826 55-66.
827
828 Scott, A.C. Jones,T.P. 1991. Microscopical observations of Recent and fossil
829 charcoal. Microscopy and Analysis 24, 13-15
830

831 Scott, A.C., Jones, T. J., 1994. The nature and influence of fires in Carboniferous
832 ecosystems. Palaeogeography, Palaeoclimatology, Palaeoecology 106, 91-112.
833
834 Schmidt, M.W.I., Skjemstad, J.O., Czimczik, C.I., Glaser, B., Prentice, K.M., Gelinas
835 Y., Kuhlbusch, T.A.J., 2001. Comparative analysis of black carbon in soils. Global
836 Biogeochemical Cycles 15, 163–167.
837
838 Sima-Ella, E., Yuan, G., Mays, T., 2005. A simple kinetic analysis to determine the
839 intrinsic reactivity of coal char. Fuel 84, 1920–1925.
840
841 Stach, E., Mackowsky, M.-Th., Teichmüller, M., Taylor, G.H., Chandra, D.,
842 Teichmüller, R., 1982. Stach's Textbook of Coal Petrology, Gebrüder Borntraeger,
843 Berlin-Stuttgart.
844
845 Steelman, K.L., Rickman, R., Rowe, M.W., Boutton, T.W., Russ, J., Guidon, N.,
846 2002. Accelerator mass spectrometric radiocarbon ages of an oxalate accretion and
847 rock paintings at Toca do Serrote da Bastiana, Brazil. In: Jakes, K.A. (Ed.)
848 Archaeological Chemistry VI: Materials, Methods, and Meaning, #831, American
849 Chemical Society, Washington, DC, pp. 22–35.
850
851 Stinson, K. J., Wright, H. A., 1969. Temperatures of Headfires in the Southern Mixed
852 Prairie of Texas. Journal of Range Management 22, 169-174.
853
854 Stronach, N. R. H., McNaughton, S.J., 1989. Grassland fire dynamics in the
855 Serengeti ecosystem, and a potential method of retrospectively estimating fire energy.
856 Journal of Applied Ecology 26, 1025-1033.
857
858 Swift, L.W. Jr., Elliott, KJ., Ottmar, R.D., Vihnanek, R.E., 1993. Site preparation
859 burning to improve southern Appalachian pine-hardwood stands: fire characteristics
860 and soil erosion, moisture, and temperature. Canadian Journal of Forest Research 23,
861 2242-2254.
862

Trompowsky, P. M., Benites, V. M., Madari, B. E., Pimenta, A.S., Hockaday, W. C., Hatcher, P. G., 2005 Characterization of humic like substances obtained by chemical oxidation of eucalyptus charcoal, Organic Geochemistry 36, 1480-1489.

Tuinstra, F., Koenig, J. L., 1969. Characterization of Graphite Fiber Surfaces with Raman Spectroscopy J. Chem. Phys. 53, 1126–1130.

Tuinstra, F., Koenig,, J. L. 1970. Raman Spectrum of Graphite. Journal of Chemical Physics 53, 1126.

Turney, C. S. M., Wheeler, D., Chivas A. R., 2006. Carbon isotope fractionation in wood during carbonization. Geochimica et Cosmochimica Acta 70, 960–964.

Van Krevelen, D., 1950. Graphical–statistical method for the study of structure and reaction process of coal. Fuel 29, 269–284.

Walker, P.L. Jr., Rusinko, F. Jr., Austin, L. G., 1959. In: Eley, D.D., Selwood, P.W., Weisz, P.B. (Ed.s), Advances in Catalysis, 11, Academic Press, New York , p. 164

Werts S. P., Jahren A. H., 2007 Estimation of temperatures beneath archaeological campfires using stable isotopic composition of soil organic matter. Journal of Archaeological Science 34, 850-857.

Williams P. T., Besler, S., 1996. The influence of temperature and heating rate on the slow pyrolysis of biomass. Renewable Energy 7, 233-250.

Wolbach, W.S., Anders, E., 1989. Elemental carbon in sediments: Determination and spectroscopic analysis in the presence of kerogen. Geochimica et Cosmochimica Acta 53,1637–1647.

Figures:

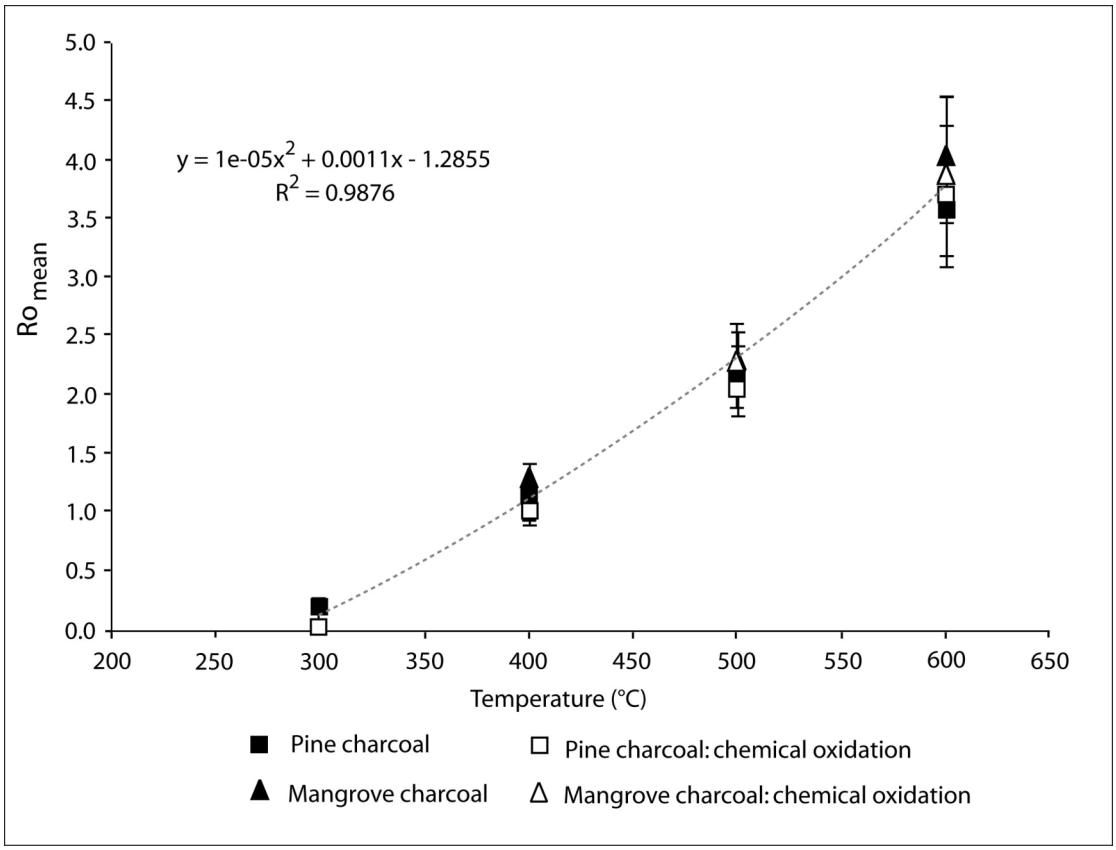

Figure 1: Mean random reflectance under oil (Ro_{mean}) measurements and standard deviations for Fr_{char} samples prior to and following chemical oxidation. The dotted line shows the correlation between Ro_{mean} and production temperature for measured samples. Note that graphical data for different sample types overlap at 300°C, 400°C and 500°C, meaning some data points are obscured at these temperatures.

Figure 2: Thin section (Light Micrograph) of *Pinus* (P-300) Fr_{char} after oxidation showing lightening of colour in the cell walls in a few outer cell layers. The outermost surface shows damage caused during production of the wood block (see methods).

Figure 3: TEM images of P-300 *Pinus* Fr_{char}, focussing upon the sample area that underwent lightening during oxidation (see text and Figure 2). A and B: Unoxidized outer cell walls, C and D: Outer cell walls after 24 hours $K_2Cr_2O_7$ oxidation. Comparison of images shows no significant structural changes following oxidation.

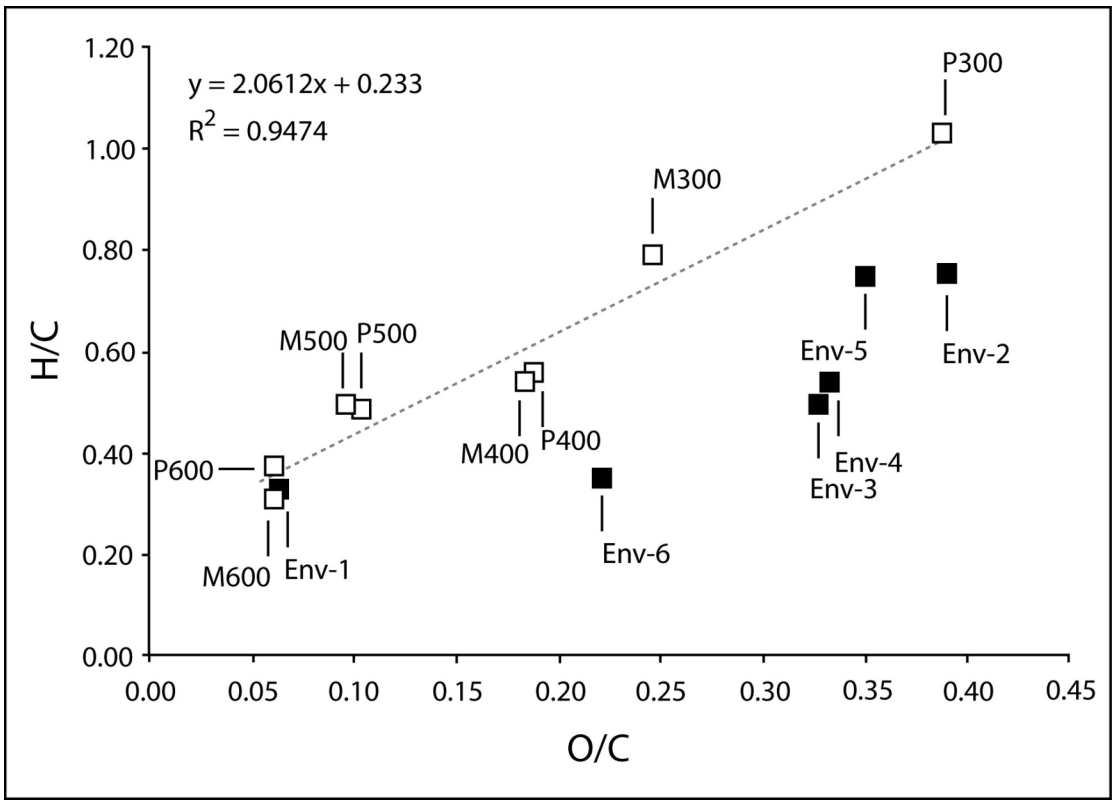

908

909 Figure 4: Van Krevelan diagram of Fr_{char} (white squares) and Env_{char} (black squares)
910 showing atomic ratios of O/C and H/C. The dotted line shows the linear correlation
911 between O/C and H/C ratios in the Fr_{char} samples, where increases in both these
912 parameters occur with increasing production temperature.

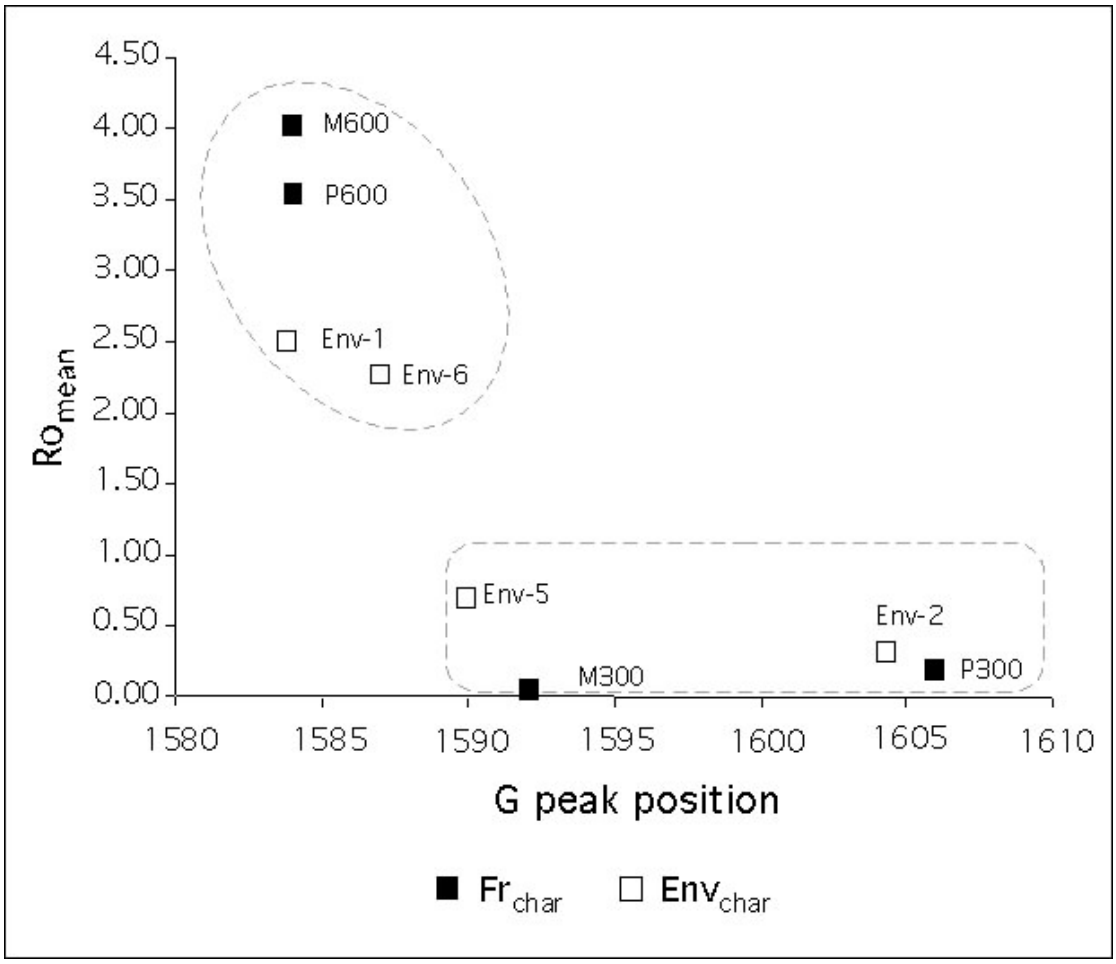

913

914 Figure 5: Ro_{mean} versus Raman G peak position for both Fr_{char})and Env_{char} samples,
915 showing the relationship between increasing G peak position and decreasing Ro_{mean}
916 values in both sample types. Analysed samples fall into two groups (indicated by
917 dashed boxes), where high Ro_{mean} corresponds to lower G peak position and vice
918 versa.

919
920
921

Tables

Table 1: Details of modern analogue (Fr_{char}) and environmental (Env_{char}) charcoal samples used in this study.

Table 2: Ro_{mean} and measurement standard deviations for charcoal samples based on 100 measurements of reflectance across the sample surface and assessments of charcoal production temperatures derived from Ro_{mean} for both Fr_{char} and Env_{char} samples. Mass losses and Ro_{mean} values following $K_2Cr_2O_7$ oxidation treatment are given for the Fr_{char} samples.

Table 3: Content of carbon, oxygen and hydrogen (by weight %) derived via elemental analysis of Fr_{char} and Env_{char} samples, together with calculated atomic O/C and H/C ratios for these samples.

Table 4: Results of Raman spectroscopic measurements for high and low temperature Fr_{char} and selected Env_{char} samples detailing the width and position of the G peak for organized (i.e. graphite-like) carbon and the D peak for disorganized carbon within the samples.

Table 5: Volatile content, Burnout Time to 90% and composite first order rate constant calculated on the basis of TGA analysis for high and low temperature Fr_{char} and selected Env_{char} samples

Modern analogue charcoal samples (Fr_{char})			**Environmental charcoal samples (Env_{char})**		
Sample code	**Species**	**Temperature (°C)**	**Sample code**	**Site**	**Location**
P-300	*Pinus sylvestris*	300	**Env-1**	Maninjau	Sumatra
P-400	*Pinus sylvestris*	400	**Env-2**	Faial island	Azores
P-500	*Pinus sylvestris*	500	**Env-3**	Langanes	Iceland
P-600	*Pinus sylvestris*	600	**Env-4**	Höskulsstaðir	Iceland
M-300	*Rhizophora apiculata*	300	**Env-5**	Toca da Bastiana	Brazil
M-400	*Rhizophora apiculata*	400	**Env-6**	Oursi-hubeero	Burkino Faso
M-500	*Rhizophora apiculata*	500			
M-600	*Rhizophora apiculata*	600			

Table 1: Details of modern analogue (Fr_{char}) and environmental (Env_{char}) charcoal samples used in this study.

Sample	Ro_{mean}	standard deviation (σ)	Mean temperature calculated from Ro (°C)	Mass loss during oxidation (wt %)	Ro_{mean} Following $K_2Cr_2O_7$ oxidation	standard deviation (σ)
Env-1	2.51	0.45	515	-	-	-
Env-2	0.31	0.24	320	-	-	-
Env-3	0.70	0.24	361	-	-	-
Env-4	0.60	0.31	351	-	-	-
Env-5	0.70	0.21	361	-	-	-
Env-6	2.26	0.33	497	-	-	-
M-600	4.01	0.52	617	<1	3.87	0.41
M-500	2.27	0.26	498	0	2.28	0.32
M-400	1.26	0.14	415	2	1.07	0.16
M-300	0.03	0.01	287	36	-	-
P-600	3.54	0.36	587	<1	3.68	0.6
P-500	2.15	0.25	488	<1	2.04	0.22
P-400	1.13	0.13	403	0	1.01	0.12
P-300	0.19	0.08	306	73	-	-

Table 2: Ro_{mean} and measurement standard deviations for charcoal samples based on 100 measurements of reflectance across the sample surface and assessments of charcoal production temperatures derived from Ro_{mean} for both Fr_{char} and Env_{char} samples. Mass losses and Ro_{mean} values following $K_2Cr_2O_7$ oxidation treatment are given for the Fr_{char} samples.

Sample	C (wt %)	%O (wt %)	%H (wt %)	Atomic O/C ratio	Atomic H/C ratio
P-300	59	31	5	0.39	1.05
P-400	73	18	3	0.19	0.57
P-500	81	11	3	0.10	0.49
P-600	85	7	2	0.06	0.37
M-300	68	22	5	0.25	0.79
M-400	74	18	3	0.18	0.54
M-500	80	10	3	0.10	0.50
M-600	83	7	2	0.06	0.31
Env-1	82	7	2	0.06	0.31
Env-2	59	31	4	0.39	0.75
Env-3	63	27	3	0.33	0.50
Env-4	61	27	3	0.33	0.54
Env-5	58	27	4	0.35	0.75
Env-6	68	20	2	0.22	0.35

Table 3: Content of carbon, oxygen and hydrogen (by weight %) derived via elemental analysis of Fr_{char} and Env_{char} samples, together with calculated atomic O/C and H/C ratios for these samples.

Sample	I_G width (cm^{-1})	I_G position (cm^{-1})	D width (cm^{-1})	D position (cm^{-1})
P-300	260.1	1606	299.47	1342.86
P-600	111.5	1584	261.17	1333.00
M-300	334.0	1592	303.75	1314.98
M-600	115.1	1584	285.12	1337.53
Env-1	116.1	1583.8	267.12	1343.20
Env-2	221.2	1604.4	380.32	1361.49
Env-5	165.5	1590	322.80	1351.31
Env-6	134.9	1587	280.00	1341.83

Table 4: Results of Raman spectroscopic measurements for high and low temperature Fr_{char} and selected Env_{char} samples detailing the width and position of the G peak for organized (i.e. graphite-like) carbon and the D peak for disorganized carbon within the samples.

Sample	Volatile content (%)	Burnout Time to 90% (min)	Sample	Composite first order rate constant (5-95% C Burnout) min^{-1}
P-300	49	5.9	**P-300**	0.529
P-600	7	7.3	**P-600**	0.429
M-300	31	7.4	**M-300**	0.381
M-600	6	9.8	**M-600**	0.339
Env-1	7	10.8	**Env-1**	0.314
Env-2	34	6.8	**Env-2**	0.439
Env-3	28	7.8	**Env-3**	0.413
Env-4	28	6.3	**Env-4**	0.531
Env-5	41	6.8	**Env-5**	0.467
Env-6	19	8.5	**Env-6**	0.362

Table 5: Volatile content, Burnout Time to 90% and composite first order rate constant calculated on the basis of TGA analysis for high and low temperature Fr_{char} and selected Env_{char} samples